RESEARCH COMMUNICATION

Fate of haem iron in the malaria parasite *Plasmodium falciparum*

Timothy J. EGAN*[1], Jill M. COMBRINCK†, Joanne EGAN†, Giovanni R. HEARNE‡, Helder M. MARQUES§, Skhumbuzo NTENTENI‡, B. Trevor SEWELL‖, Peter J. SMITH†, Dale TAYLOR†, Donelly A. VAN SCHALKWYK† and Jason C. WALDEN†

*Department of Chemistry, University of Cape Town, Private Bag, Rondebosch 7701, South Africa, †Department of Medicine, Division of Pharmacology, University of Cape Town, Private Bag, Rondebosch 7701, South Africa, ‡School of Physics, University of the Witwatersrand, PO Wits 2050, Johannesburg, South Africa, §School of Chemistry, University of the Witwatersrand, PO Wits 2050, Johannesburg, South Africa, and ‖Electron Microscope Unit, University of Cape Town, Private Bag, Rondebosch 7701, South Africa

Chemical analysis has shown that *Plasmodium falciparum* trophozoites contain $61 \pm 2\%$ of the iron within parasitized erythrocytes, of which $92 \pm 6\%$ is located within the food vacuole. Of this, $88 \pm 9\%$ is in the form of haemozoin. ^{57}Fe-Mössbauer spectroscopy shows that haemozoin is the only detectable iron species in trophozoites. Electron spectroscopic imaging confirms this conclusion.

Key words: haemozoin, Mössbauer spectroscopy, electron spectroscopic imaging.

INTRODUCTION

During its pathogenic intra-erythrocytic stage, the malaria parasite ingests host haemoglobin into an acidic food vacuole (FV) [1]. Here, globin is digested by a series of protease enzymes [2], and haem is released and oxidized to haematin, which is potentially toxic to the parasite. It has long been known that haemozoin (malaria pigment), present in the FV, contains ferrihaem in a highly insoluble form [3]. Recently, it was shown to be a microcrystalline cyclic dimer of ferrihaem [4]. Nonetheless, it has never been proven that incorporation into haemozoin is the main fate of haem iron, and the identity and distribution of major iron species in the parasite is currently unknown. Indeed, two recent studies have suggested that, owing to chemical degradation of haematin, more than 70% of the iron may be released in either the parasite cytosol [5] or the FV [6], although the resulting iron species were not identified. According to the hypothesis of Ginsburg et al. [5], haematin is degraded by glutathione in the parasite cytosol, whereas according to Loria et al. [6] degradation occurs through the action of H_2O_2 produced in the FV as a result of autoxidation of ferrohaem.

Given that important antimalarials apparently target haematin within the FV [7–12], the fate of this haem iron is of considerable interest, both from the point of view of the fundamental biochemistry of the FV and in the design of new antimalarials. For this reason, we have undertaken chemical analysis of the total elemental iron content of unparasitized red cells, parasitized red cells, isolated trophozoites, FVs and haemozoin to determine its distribution among these compartments. We have also performed Mössbauer spectroscopy on freeze-dried trophozoites to identify the iron species present in the parasite, and we have used electron spectroscopic imaging (ESI) with transmission electron microscopy (TEM) to visualize directly the distribution of elemental iron within the parasite. We show unequivocally that the overwhelming fate of haem is incorporation into haemozoin within the FV.

MATERIALS AND METHODS

All materials used were of the highest grade of purity available. The preparation of synthetic β-haematin was carried out exactly as described by us previously [10], except that the reaction was performed for 1 h instead of 30 min. Parasites were grown in synchronous culture, as described previously [13,14]. Parasitized erythrocytes were enriched to $> 90\%$ parasitaemia by sorbitol/Percoll-gradient centrifugation, as described by Aley et al. [15]. Trophozoites were isolated by saponin lysis of the erythrocytes from the parasite culture. Inspection by visible microscopy of Giemsa-stained parasites was performed to confirm the integrity of the isolated trophozoites. FVs were isolated from trophozoites and purified as described previously [16]. Lastly, haemozoin was isolated from FVs by freeze–thaw lysis of a known concentration of FVs, and was washed extensively with water.

Iron determination in each case was performed with a colorimetric assay using ferrozine [17]. The method involves the liberation of iron from all complexes (including haem) with H_2O_2, allowing total iron determination. For each cell fraction investigated, an approx. 0.1% (v/v) suspension of cells or vacuoles was prepared from the stock suspension and counted using a haemocytometer. Once this count was known, four or five different concentrations were prepared by dilution of the stock, iron measurements were performed on each preparation in triplicate and the iron mass per cell was calculated. The iron measurements thus represent the average of at least 12 readings.

For Mössbauer spectroscopy, approx. 5 ml of packed trophozoites were harvested over a period of 2 months and stored at 203 K before freeze-drying at 78 K. Samples were clamped in thin Teflon holders and top-loaded into a Janis liquid-helium cryostat. A 10 mCi ^{57}Co(Rh) source was used in conjunction with a $KrCO_2$ proportional counter using a Wissel constant acceleration drive. Source and sample were in close proximity and at nearly the same temperature. Temperatures were stabilized to within 0.2 K for extended periods with a Lakeshore temp-

Abbreviations used: ESI, electron spectroscopic imaging; FV, food vacuole; TEM, transmission electron microscopy.

[1] To whom correspondence should be addressed (e-mail tegan@science.uct.ac.za).

erature controller and calibrated Si diode temperature sensor close to the sample. For the β-haematin sample, approx. 25 mg/cm² (approx. 9 mg/cm² of Fe) was used, whereas for the trophozoites approx. 125 mg/cm² was loaded. Calibration was achieved with a natural iron absorber held at room temperature. Isomer shifts are quoted relative to α-Fe at room temperature. Each spectrum and its mirror image was acquired in 1024 channels, and then folded to remove baseline curvature. Adjacent channels were added to reduce statistical scatter, before theoretical fitting was effected on the final processed spectrum in 256 channels using the Mössbauer fitting program NORMOS. Each spectrum was fitted with a Lorentzian doublet, relative intensities of which were allowed to vary to account for asymmetry arising from temperature-dependent relaxation effects [18].

Samples for TEM/ESI were prepared by fixing in 5% (v/v) glutaraldehyde in PBS for 10 min at room temperature, washing with PBS and resuspending in 2.5% glutaraldehyde overnight at 4 °C. They were then post-fixed in 1% (w/v) OsO_4 in PBS for 1 h, washed with PBS and then stained with 1% (w/v) uranyl acetate. After washing with distilled water and suspending in 1% (w/v) agar, the solidified sample was cut into 1 mm cubes and dehydrated with a series of 10 ethanol/water solutions [30–95% (v/v) ethanol, 5 min each, followed twice by 100% ethanol for 10 min]. Ethanol was replaced by acetone, gradually followed by Spurr's epoxy resin (Wirsam, Johannesburg, South Africa) over 2 days and allowed to harden over 16 h. Sections were cut with a Reichert Ultracut S ultratome using glass knives and picked up on 200 mesh square copper grids. TEM and ESI were performed on a LEO 912 AB transmission electron microscope by collecting 512 × 512 pixel energy-filtered images on a Tiedtz charge-coupled-device camera. The iron-distribution image is the difference between an image collected at an energy offset of 722 eV corresponding to the Fe L_{II} absorption edge using a slit width of 19 eV and a calculated background image. Background at 722 eV was computed by extrapolating from two images collected at 655 eV and 687 eV using a three-window power law [19].

RESULTS AND DISCUSSION

Scheme 1 shows our approach to the determination by chemical analysis of iron contained within the various structures within parasitized erythrocytes. The mass of iron found is also shown. Elemental iron content within unparasitized erythrocytes is in excellent agreement with the accepted range of 90–111 fg/cell [20]. Parasitized red cells contain the same quantity of iron, demonstrating that there is no significant net loss or gain of iron as a result of the presence of the parasite within the erythrocyte. Isolated trophozoites contain 61 ± 2% of the iron within the parasitized cell. This agrees well with our finding that 62 ± 13% (mean value ± S.D.) of the haemoglobin had been digested in the parasitized red blood cells, as determined by SDS/PAGE (15% gels) quantified by Coomassie Blue staining. It also agrees well with previous reports suggesting variously that up to 65% of the haemoglobin is digested [21], that 72–80% has been digested at the trophozoite stage [5], and that 75% has been digested by the time the schizont stage is reached [6]. We find that FVs contain 92 ± 6% of this parasite iron. This value directly contradicts the

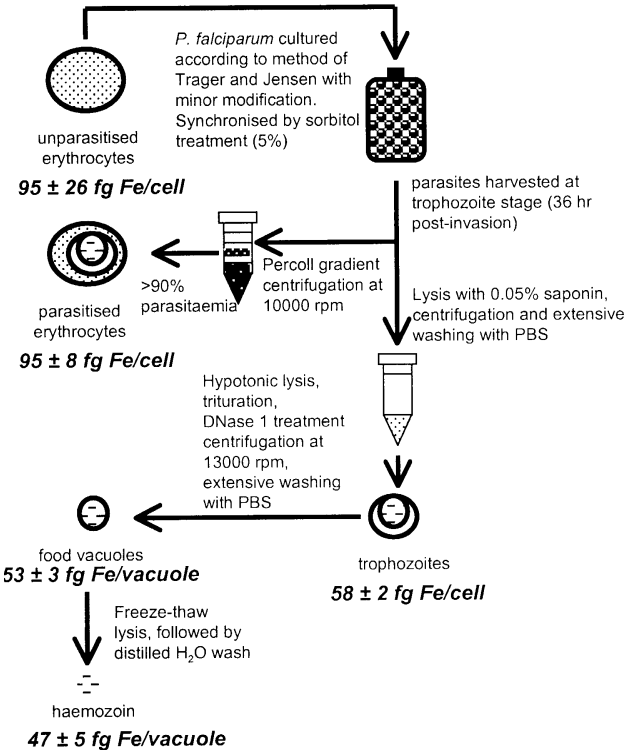

Scheme 1 Iron content within unparasitized red blood cells, parasitized red blood cells, isolated trophozoites, FVs and haemozoin

Schematic diagram of the procedures used to determine iron content within parasitized and unparasitized erythrocytes, trophozoites, FVs and haemozoin. Iron masses per cell or per vacuole are shown.

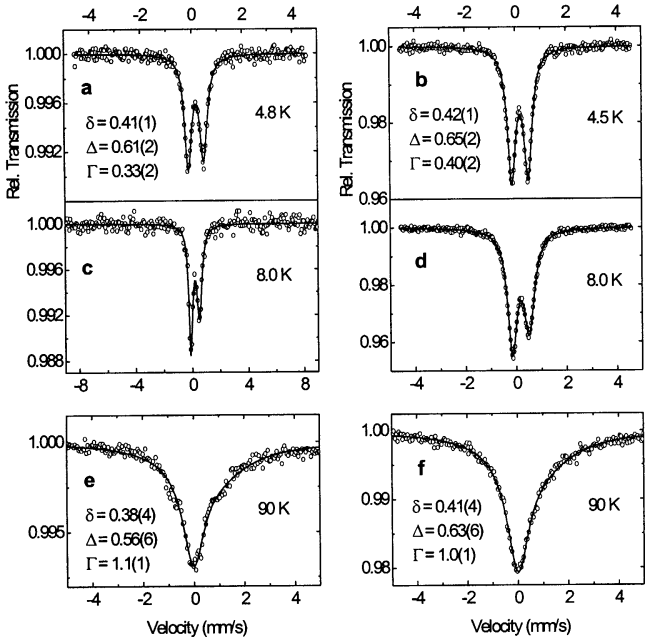

Figure 1 Mössbauer spectra of freeze-dried trophozoites (a, c and e) and β-haematin (b, d and f)

The fitted isomer shift (δ), quadrupole splitting (Δ) and linewidth (Γ), all in mm/s (the last digit in parentheses is the S.D.), are shown in the spectra. Fitted parameters at 8 K are all within the uncertainty of the values obtained at lower temperature. All features of the spectra and fitted parameters are in excellent agreement with those reported for β-haematin by Bauminger et al. [28].

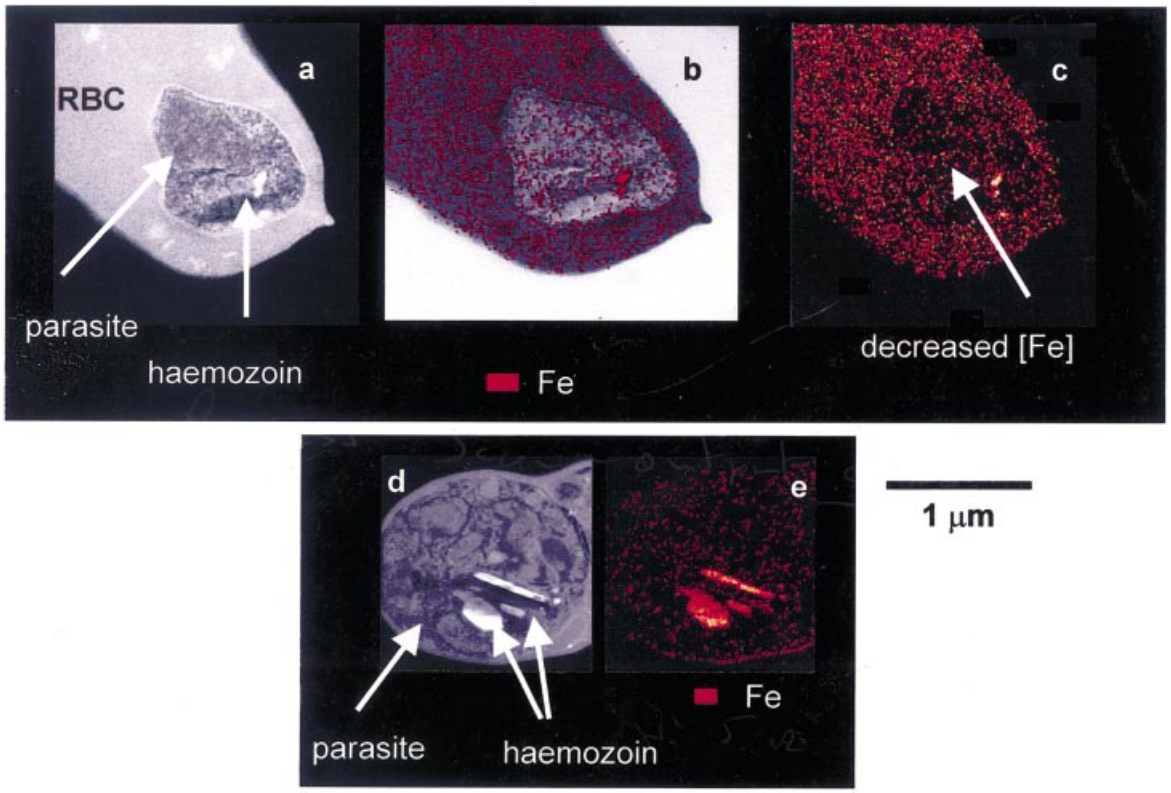

Figure 2 TEM and ESI of *Plasmodium falciparum* showing the distribution of elemental iron within a trophozoite and a blood schizont

(**a**) TEM of a trophozoite-infected erythrocyte overlaid with the distribution of iron determined by ESI (**b**). (**c**) The iron distribution alone, demonstrating that it is concentrated in haemozoin crystals within the trophozoite (small white objects in the TEM image). The rest of the parasite is devoid of iron compared with the reference level in the erythrocyte cytoplasm. (**d**) TEM of a schizont-infected erythrocyte and distribution of elemental iron (**e**). The iron distribution coincides exactly with haemozoin crystals.

hypothesis that more than 70 % of the haematin is degraded outside the FV, with its iron being deposited into the parasite cytosol [5]. Finally, 88 ± 9 % of the FV iron is recovered in the haemozoin pellet, suggesting that this material is the major iron species in the parasite.

Owing to inherent uncertainties in the counting of cells, as well as the various fractionation steps, the variance in the above data is relatively large. This means that the 95 % confidence interval for the fraction of parasite iron contained within the FV spans the range 80–100 %, and for that in the form of haemozoin it ranges from 70–100 % of the vacuolar iron. It is also potentially possible for highly insoluble non-haem iron species (such as hydrated iron oxides) to co-precipitate with haemozoin and to be recovered with it, or possibly even to adhere non-specifically to cellular components such as membranes. This introduces further uncertainty into the value obtained for haemozoin. We therefore performed ^{57}Fe-Mössbauer spectroscopy on trophozoites in order to identify directly and unequivocally the iron species within the parasite. These spectra were compared with those of synthetic haemozoin (β-haematin), prepared by a method that we have described previously [10], with the minor modification that the synthesis reaction was allowed to proceed for 1 h instead of 30 min. The spectra are shown in Figure 1. Trophozoites had to be freeze-dried in order to avoid strong attenuation of the signal by water. As can be seen, the Mössbauer spectra of freeze-dried trophozoites are identical with those of β-haematin except for the larger background scatter. This arises from the lower quantity of iron-containing material present in the biological sample. No peaks other than the central resonance (quadrupole) doublet can be discerned at the lowest temperatures. In particular, there are no peaks characteristic of haematin that we have previously shown are easily resolved from those of β-haematin [22]. Nor are there characteristic sextet (magnetic) spectral features typical of Fe(III)-oxide/hydroxide species [23] (including ferritin below 30 K [24]), as confirmed by a spectrum collected over an extended velocity range (Figure 1c), where no additional peaks are seen in the wings of the resonance profile. The temperature-dependence of the trophozoite spectrum is also identical with that of β-haematin, exhibiting a large increase in the asymmetry of the resonance doublet with rising temperature from electronic relaxation effects [18]. The inescapable conclusion arising from these data is that haemozoin (β-haematin) is the only detectable iron species within the freeze-dried trophozoite. From the magnitude of the statistical scatter in the data we can confidently state that at least 95 % of the iron observed within the trophozoite is incorporated into haemozoin. Although it is likely that freeze-drying will break down cell membranes and has the potential to disturb species within the parasite, it is not possible for haemozoin to be re-assembled from chemically degraded haematin. This means that any such degradation processes that may occur must be, at most, a minor component of the overall haematin processing in the parasite. The low temperatures or solvent-free conditions present during and after freeze-drying would also not favour conversion of haematin into

haemozoin. The observed fraction of haemozoin iron in the sample thus almost certainly is representative of that in the live trophozoite.

Further support for this distribution of iron species within the parasite comes from TEM with ESI [25]. Figures 2(a)–2(c) show a TEM of a trophozoite within an erythrocyte, together with an image of the distribution of elemental iron. It is immediately apparent from Figure 2(c) that considerable iron is associated with haemozoin crystals within the parasite as expected, but the rest of the parasite is largely devoid of iron. Haemoglobin iron within the erythrocyte cytosol, on the other hand, is clearly visible. Given that approx. 60% of the total iron is within the parasite and that the parasite has a lower volume than the erythrocyte, if this iron were dissolved or deposited throughout its cytosol or throughout the FV, then the iron concentration in these compartments would be markedly higher than in the erythrocyte cytosol. In a schizont (Figures 2d and 2e), very little iron is present within either the erythrocyte cytosol or the parasite. The haemozoin crystals, however, show up strongly. This distribution of iron is in complete accordance with the chemical elemental iron analyses and the Mössbauer spectroscopy data.

We conclude that the fate of more than 95% of the haem iron released from host haemoglobin within the D10 strain of *Plasmodium falciparum* is incorporation into haemozoin. Formation of this highly insoluble, crystalline material thus represents the major haem-detoxification pathway of the parasite. We cannot exclude the possibility that a small fraction of this haem ($< 5\%$) may be degraded. Such processes could, for example, provide the parasite's iron requirement, but definitive evidence in this regard is lacking. The results do not support suggestions that more than 70% of the haem iron is released from the porphyrin [5,6]. These earlier studies were based on measurements of total haematin concentration in the parasite that could account for only 30% or less of the non-haemoglobin iron. We suspect that this discrepancy arose from the use of the haematin Soret band intensity as a means to quantify haematin. Owing to the known ability of haematin to exist in different aggregation states in basic solution [26] and the potential effects of ligands on the intensity and position of the Soret band of Fe(III) porphyrins [27], this method of quantification may be unreliable in the presence of the biological matrix. In addition, base extraction of haematin from parasite material may be incomplete. Our findings have several implications for the probable mechanism of action of antimalarials, such as chloroquine. Given the minor or even non-existent role of haematin degradation in the parasite, it would seem unlikely that inhibition of such processes represents the mechanism of drug action. Secondly, large quantities of free haematin are not present in the parasite, but the ^{57}Fe-Mössbauer data do not exclude the presence of low concentrations of non-haemozoin forms of iron within the parasite, not exceeding 5% of the total iron content. Thus we cannot exclude the presence of up to 5% haematin in the parasite. At the very least, there must be a transient (possibly steady-state) pool of haematin produced upon oxidation of haem, but prior to its incorporation into haemozoin. A portion of this may well be available as a target for such drugs. Lastly, haemozoin formation is clearly a major pathway within the FV, and so proposals that the mechanism of action of these drugs involve its inhibition [9–12] appear feasible, at least from the point of view of importance of the process to the parasite.

We thank Mr Mohammed Jaffer (Electron Microscope Unit, University of Cape Town, South Africa) for assistance with the preparation of samples for TEM, and Dr Alvaro de Sousa (School of Chemistry, University of the Witwatersrand, South Africa) for assistance with freeze-drying. TEM with ESI was kindly performed at LEO Elektronenmikroskopie GmbH by Mr Volker Seybold. We thank the National Research Foundation (Pretoria, South Africa), the University of Cape Town and the University of the Witwatersrand for financial support.

REFERENCES

1 Aikawa, M., Hepler, P. K., Huff, C. G. and Sprinz, H. (1966) Feeding mechanisms of avian malarial parasites. J. Cell Biol. **28**, 355–373
2 Banerjee, R., Liu, J., Beatty, W., Pelosof, L., Klemba, M. and Goldberg, D. E. (2002) Four plasmepsins are active in the *Plasmodium falciparum* food vacuole, including a protease with an active-site histidine. Proc. Natl. Acad. Sci. U.S.A. **99**, 990–995
3 Brown, W. H. (1911) Malarial pigment (so-called melanin): its nature and mode of production. J. Exp. Med. **13**, 290–299
4 Pagola, S., Stephens, P. W., Bohle, D. S., Kosar, A. D. and Madsen, S. K. (2000) The structure of malaria pigment (β-haematin). Nature (London) **404**, 307–310
5 Ginsburg, H., Famin, O., Zhang, J. and Krugliak, M. (1998) Inhibition of glutathione-dependent degradation of heme by chloroquine and amodiaquine as a possible basis for their antimalarial mode of action. Biochem. Pharmacol. **56**, 1305–1313
6 Loria, P., Miller, S., Foley, M. and Tilley, L. (1999) Inhibition of the peroxidative degradation of haem as the basis of action of chloroquine and other quinoline antimalarials. Biochem. J. **339**, 363–370
7 Mungthin, M., Bray, P. G., Ridley, R. G. and Ward, S. A. (1998) Central role of hemoglobin degradation in mechanisms of action of 4-aminoquinolines, quinoline methanols, and phenanthrene methanols. Antimicrob. Agents Chemother. **42**, 2973–2977
8 Bray, P. G., Mungthin, M., Ridley, R. G. and Ward, S. A. (1998) Access to hematin: the basis of chloroquine resistance. Mol. Pharmacol. **54**, 170–179
9 Slater, A. F. G. and Cerami, A. (1992) Inhibition by chloroquine of a novel haem polymerase enzyme activity in malaria trophozoites. Nature (London) **355**, 167–169
10 Egan, T. J., Ross, D. C. and Adams, P. A. (1994) Quinoline anti-malarial drugs inhibit spontaneous formation of β-haematin (malaria pigment). FEBS Lett. **352**, 54–57
11 Dorn, A., Stoffel, R., Matile, H., Bubendorf, A. and Ridley, R. G. (1995) Malarial haemozoin/β-haematin supports haem polymerization in the absence of protein. Nature (London) **374**, 269–271
12 Sullivan, D. J., Gluzman, I. Y., Russell, D. G. and Goldberg, D. E. (1996) On the molecular mechanism of chloroquine's antimalarial action. Proc. Natl. Acad. Sci. U.S.A. **93**, 11865–11870
13 Trager, W. and Jensen, J. B. (1976) Human malaria parasites in continuous culture. Science **193**, 673–675
14 Lambros, C. and Vanderberg, J. P. (1979) Synchronisation of *Plasmodium falciparum* erythrocyte stages in culture. J. Parasitol. **65**, 418–420
15 Aley, S. B., Sherwood, J. A., Marsh, K., Eidelman, O. and Howard, R. J. (1986) Identification of isolate-specific proteins on sorbitol-enriched *Plasmodium falciparum* infected erythrocytes from Gambian patients. Parasitology **92**, 511–525
16 Saliba, K. J., Folb, P. I. and Smith, P. J. (1998) Role for the *Plasmodium falciparum* digestive vacuole in chloroquine resistance. Biochem. Pharmacol. **56**, 313–320
17 Carter, P. (1971) Spectrophotometric determination of serum iron at the submicrogram level with a new reagent (ferrozine). Anal. Biochem. **40**, 450–458
18 Blume, M. (1967) Temperature-dependent spin-spin relaxation times: application to the Mössbauer spectra of ferric hemin. Phys. Rev. Lett. **18**, 350–358
19 Egerton, R. F. (1996) Electron Energy-Loss Spectroscopy in the Electron Microscope, 2nd edn, Plenum Press, New York, NY
20 Greendyke, R. M., Meriwether, W. A., Thomas, E. T., Flintjer, J. D. and Bayliss, M. W. (1962) Suggested revision of normal values for haemoglobin, haematocrit, and erythrocyte count in healthy adult men. Am. J. Clin. Pathol. **37**, 429–436
21 Krugliak, M., Zhang, J. and Ginsburg, H. (2002) Intraerythrocytic *Plasmodium falciparum* utilises only a fraction of the amino acids derived from digestion of host cell cytosol for the biosynthesis of its proteins. Mol. Biochem. Parasitol. **119**, 249–256
22 Adams, P. A., Egan, T. J., Ross, D. C., Silver, J. and Marsh, P. J. (1996) The chemical mechanism of β-haematin formation studied by Mössbauer spectroscopy. Biochem. J. **318**, 25–27
23 Danon, J. (1968) ^{57}Fe: metal, alloys, and inorganic compounds. In Chemical Applications of Mössbauer Spectroscopy (Goldanskii, V. I. and Herber, R. H., eds.), pp. 159–267, Academic Press, New York, NY
24 Moshkovskii, Y. S. (1968) Applications of the Mössbauer effect in biology. In Chemical Applications of Mössbauer Spectroscopy (Goldanskii, V. I. and Herber, R. H., eds.), pp. 524–547, Academic Press, New York, NY

25 Beckers, A. L. D., De Bruijn, W. C., Gelsema, E. S., Cleton-Soeteman, M. I. and Van Eijk, H. G. (1994) Quantitative electron spectroscopic imaging in bio-medicine: methods for image acquisition, correction and analysis. J. Microsc. **174**, 171–182
26 O'Keeffe, D. H., Barlow, C. H., Smythe, G. A., Fuchsman, W. H., Moss, T. H., Lilienthal, H. R. and Caughey, W. S. (1975) Magnetic and spectroscopic probes for FeOFe linkages in hemin systems. Bioinorg. Chem. **5**, 125–147
27 Marques, H. M., Munro, O. Q., Munro, T., de Wet, M. and Vashi, P. R. (1999) Coordination of N-donor ligands by the monomeric ferric porphyrin N-acetylmicroperoxidase-8. Inorg. Chem. **38**, 2312–2319
28 Bauminger, E. R., Akkawi, M. and Blauer, G. (1999) Mössbauer studies of different types of hematin. Inorg. Chim. Acta **286**, 229–232

Received 20 May 2002; accepted 29 May 2002
Published as BJ Immediate Publication 29 May 2002, DOI 10.1042/BJ20020793